AAG2018

Advances in Architectural Geometry 2018
Chalmers University of Technology
Gothenburg, Sweden
22-25 September 2018

www.architecturalgeometry.org/aag18

Aligning principal stress and curvature directions

Davide Pellis[1], Helmut Pottmann[1]

[1] Institute of Discrete Mathematics and Geometry
Vienna University of Technology (TU Wien), Austria
davidepellis@gmail.com
pottmann@geometrie.tuwien.ac.at

Abstract

Designing freeform architectural surfaces with due regard to economic and feasibility factors is a challenging task. Rationalizing such surfaces by means of quadrilateral meshes following principal curvature lines has proven to be beneficial for manufacturing reasons, such as planar cladding panels and simplified substructure connections. On the other hand, for structural efficiency, it is convenient to ensure static equilibrium in the load bearing structure through axial forces only. It turns out that both of these goals can be reached for surfaces in membrane equilibrium where principal stress and curvature directions coincide. In this paper, we present a method for the optimization of a given shape towards stress and curvature alignment, within a workflow for the design of principal meshes in equilibrium. Our method can be applied to shapes without any geometric or topological limitation.

Key words: architectural geometry, computational design, freeform architecture, principal meshes in equilibrium, structural optimization

1 Introduction

Motivation. Principal meshes are discrete versions of principal curvature parametrizations of surfaces. This kind of meshes is particularly suitable in architecture for several reasons. First of all, faces are planar and then easily manufacturable. Moreover, the network lines are as orthogonal as possible and admit the disposition of prismatic beams that meet in the nodes with minimized geometric torsion, reducing significantly the complexity of connections. On the other hand, the edges of these meshes are charged to bear the loads within the structure. It is well known that the most efficient manner of bearing loads in a framework is through strictly axial forces. This allows the beam cross section to be used to the highest capacity and at the same time to offer the highest stiffness. Principal meshes in axial force equilibrium provide an appealing solution for the discretization of freeform architectural surfaces. However, principality and equilibrium of quad meshes turn out to be often conflicting goals. It is of interest then to provide computational tools that enable to embody geometric and static optimization since the earliest design stages.

Previous work. A significant step in mesh optimization for equilibrium comes from *thrust network analysis*, introduced by Block and Ochsendorf (2007). Vouga et al. (2012) provide a differential geometric understanding of this approach and use it for the design of planar quad meshes in equilibrium. An efficient optimization of quad meshes for equilibrium and face planarity is provided by Tang et al. (2014), but the success of this method is strongly dependent on the initial mesh connectivity. Schiftner and Balzer (2010) propose a method for planar quad-remeshing of given surfaces, initialized by principal stress lines. However, the effectiveness of this method is limited, since for a general surface, planarity of quads and the alignment with principal stress directions are often conflicting goals. A first attempt to directly design principal meshes in equilibrium was made by Sun (2016), fixing the mesh combinatorics in advance. Unfortunately, this approach rarely yields good

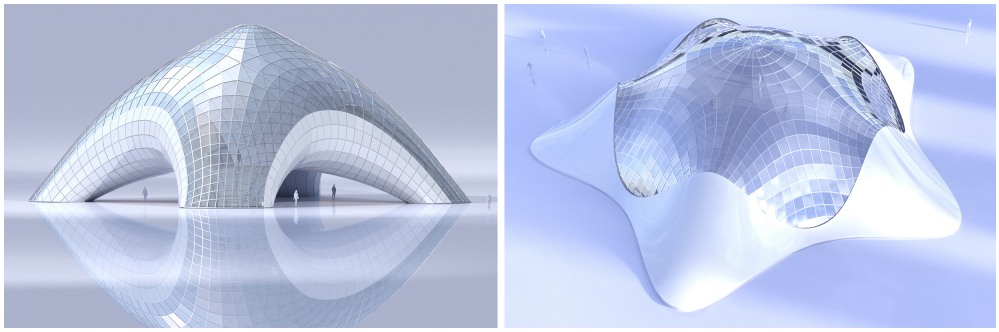

Figure 1: Architectural surfaces discretized with principal meshes in equilibrium, achieved thanks to stress and curvature alignment. Cladding can be realized with flat panels, and the substructure with prismatic beams and torsion-free nodes. At the same time, structural bending effects are minimized. The mesh on the left discretizes a non-height field shape.

convergence of optimization. The design of principal meshes in equilibrium is addressed in (Kilian et al., 2017), thanks to the alignment of principal curvature and stress directions and a subsequent quad-remeshing. However, the applicability of this method is restricted to height field shapes. We refer to the latter paper for further literature. For an introduction to principal meshes in architecture, we refer to (Pottmann et al., 2015).

Our contribution. It turns out that principal meshes in equilibrium are a discretization of membrane surfaces with coincident stress and curvature directions. In this paper, we propose a method for the optimization of a given shape towards stress and curvature alignment, within a workflow for the design of principal meshes in equilibrium. Relying on a discrete-continuous analog, we discretize a given surface with a triangular mesh, enforcing the equilibrium on its edges, and we estimate an equivalent membrane stress and curvature. We overcome in this way the shape limitations of (Kilian et al., 2017). Once the shape is optimized for stress and curvature alignment, we generate a quad mesh along the resulting directions that is post-optimized for force equilibrium and face planarity. Thanks to our initialization, we can expect convergence with minimal changes. It is noteworthy that mesh connectivity and geometry are both part of our solution.

2 Membranes and gridshells

This paper deals with meshes in equilibrium under axial forces and subject to vertical loads. We consider self-weight, dead, and static live loads lumped in forces and applied in the vertices. The resulting framework structure is a *gridshell truss*: a system of straight beams, with axes corresponding to the edges of the mesh, connected together and to the supports with frictionless pin-joints. In this paper, we refer to this model as *gridshell*. We point out here that this kind of structure, depending on its geometry, connectivity and support conditions, might be a mechanism in equilibrium. However, even if in an actual gridshell the nodes are manufactured as rigid joints for stability and safety reasons, the use of a truss model in the design stage is strongly beneficial for minimizing bending effects.

Let us consider now a refinement process that increases the density of a gridshell truss. From a mechanical point of view, at the limit of refinement the gridshell will tend to a *membrane*: a surface-like continuum that cannot support out of plane bending, and with mechanical properties derived at each point from the thickness in the normal direction. At the same time, the axial forces in the beams will tend to the *membrane stress*. For a detailed description of gridshells approaching membranes, we refer to (Mitchell, 2013).

In this paper, we rely on a discrete-continuous analog based on this refinement process to describe principal meshes in equilibrium. In the following of this section, we introduce the computational setting of continuous and discrete equilibrium, namely membranes and gridshells.

2.1 Membrane equilibrium

Let us consider a membrane $\mathscr{M}$ given by a regular surface. Away from points with a vertical tangent plane, we parametrize the surface locally as a height function $\mathscr{M}(x,y) = (x,y,z(x,y))$. If we consider only vertical loads, it is convenient to express equilibrium in the global coordinate system (x,y,z), with a vertical z axis. Let $\bar{S}$ be the tensor representing the xy projection of the membrane stresses. The horizontal and vertical equilibrium, respectively, are expressed by

$$\operatorname{div}(\bar{S}) = \mathbf{0}, \quad \operatorname{div}(\bar{S}\nabla z) = \rho.$$

Here divergence of a matrix is applied to its columns, and $\rho(x,y)$ is the vertical load per unit xy area (Angelillo and Fortunato, 2004; Vouga et al., 2012).

The horizontal component of the equilibrium can be expressed by the existence of an Airy stress potential $\phi(x,y)$. The stress tensor $\bar{S}$ is then given by the adjoint Hessian of ϕ:

$$\bar{S} = \widetilde{\nabla}^2\phi = \begin{pmatrix} \phi_{,yy} & -\phi_{,xy} \\ -\phi_{,xy} & \phi_{,xx} \end{pmatrix},$$

where with comma we denote partial derivatives, and with over-tilde the adjoint matrix operation. Let $\mathbb{I}$ be the first fundamental form of $\mathscr{M}(x,y)$. The *principal stresses* are then given by the eigenvalues of $\Delta^{1/2}\mathbb{I}^{-1}\nabla^2\phi$, where $\Delta = \det(\mathbb{I})$. The corresponding eigenvectors define the *principal stress directions* of $\mathscr{M}(x,y)$. For further details we refer to (Kilian et al., 2017).

We can consider the Airy stress potential as a surface $z = \phi(x,y)$ in *isotropic space*. This is a 3D space with a preferred direction along the z axis, and where distances are measured in the xy plane. The Hessian of ϕ plays here the role of shape operator, and its eigenvalues are the *isotropic principal curvatures*. These correspond to the eigenvalues of $\bar{S}$ along the swapped eigenvectors. For an introduction to isotropic geometry, we refer to (Pottmann and Liu, 2007).

2.2 Gridshell equilibrium

Let M be a three dimensional gridshell truss, with members corresponding to the edges of a mesh. We consider vertical loads applied in the vertices $\mathbf{v}_i = (x_i, y_i, z_i)$ and support conditions given along the boundary. The force $\mathbf{f}_{ij}$ exerted by the oriented bar $\mathbf{e}_{ij} = \mathbf{v}_i - \mathbf{v}_j$ on the vertex $\mathbf{v}_i$ can be expressed as $w_{ij}(\mathbf{v}_i - \mathbf{v}_j)$, where w_{ij} is the axial force per unit bar length or *force density*, and where positive values of w_{ij} indicate compression. Let A_i be the area of influence at $\mathbf{v}_i$. If the system is in equilibrium, at each unsupported vertex $\mathbf{v}_i$ the horizontal and vertical force balance gives, respectively,

$$\sum_{j\sim i} w_{ij}(\bar{\mathbf{v}}_i - \bar{\mathbf{v}}_j) = \mathbf{0}, \quad \sum_{j\sim i} w_{ij}(z_i - z_j) = \rho_i A_i, \tag{1}$$

where $\bar{\mathbf{v}}_i, \bar{\mathbf{v}}_j$ are the xy projections of the points $\mathbf{v}_i, \mathbf{v}_j$, and ρ_i is the vertex-wise load per unit area. With $j\sim i$ we denote all the vertices j connected with the vertex i.

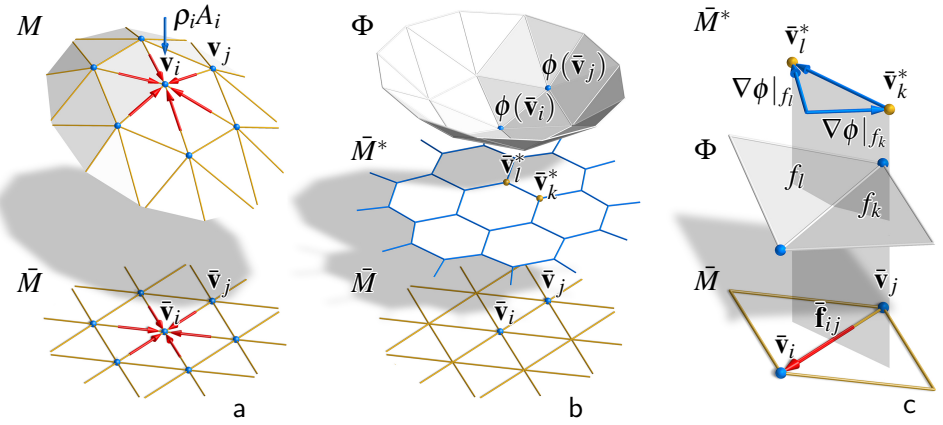

*Figure 2: Gridshell equilibrium. **(a)** A portion of a gridshell M under vertical load and its projection into the xy plane $\bar{M}$. **(b)** The horizontal equilibrium yields a force dual mesh $\bar{M}^*$ with edges given by the forces acting in the correspondent primal edges of $\bar{M}$ rotated by 90 degrees, as shown by Maxwell (1872). We can construct an Airy polyhedron Φ with face gradients given by the coordinates of the corresponding dual vertex of $\bar{M}^*$. **(c)** By construction, the magnitudes of the forces in the bars $\bar{\mathbf{v}}_i - \bar{\mathbf{v}}_j$ are given by the isotropic angles between the adjacent faces on Φ. The isotropic angle can be seen as the change in slope between two faces of Φ when traversed orthogonally to $\bar{\mathbf{v}}_i - \bar{\mathbf{v}}_j$.*

Let us now consider the projection of the structure in the xy plane, denoted as $\bar{M}$. Let $\bar{\mathbf{f}}_{ij}$ be the xy projections of the forces $\mathbf{f}_{ij}$. Since $\bar{M}$ is a 2D system in horizontal equilibrium under boundary loads (given by the xy projections of the support reactions), the forces $\bar{\mathbf{f}}_{ij}$ acting on each vertex $\bar{\mathbf{v}}_i$ can be arranged in a planar closed cycle. We can build thus a reciprocal diagram $\bar{M}^*$, combinatorially dual to $\bar{M}$, whose edges are given by the forces acting in the corresponding primal edge. For convenience, we represent this dual diagram rotated by 90 degrees clockwise in the xy plane, as shown in Figure 2b.

We can now construct a polyhedral stress potential $\Phi = (x, y, \phi(x,y))$, whose edges and vertices coincide in the xy projection to the primal truss $\bar{M}$, in the following way. Let us denote as f_k the faces of Φ, and let $\bar{\mathbf{v}}_k^* = (x_k^*, y_k^*)$ be the corresponding dual vertices of $\bar{M}$. Hence, each face f_k of Φ lies on a plane with gradient $\nabla\phi|_{f_k} = (x_k^*, y_k^*)$. The closure of each face of $\bar{M}^*$ ensures the closure of the polyhedron Φ turning around the corresponding primal vertex. This construction is uniquely defined up to vertical translations and shearing. For further details we refer to (Fraternali, 2010) and (Vouga et al., 2012).

Let f_k, f_l be the faces of Φ meeting at the oriented edge with projection $\bar{\mathbf{e}}_{ij}$, as shown in Figure 2c. The force $\bar{\mathbf{f}}_{ij}$, by construction, is given by $J(\nabla\phi|_{f_l} - \nabla\phi|_{f_k})$, where $J = \left(\begin{smallmatrix} 0 & -1 \\ 1 & 0 \end{smallmatrix}\right)$ is the 90 degrees counterclockwise rotation matrix in the xy plane. Denoting the xy unit edge vector as $\hat{\bar{\mathbf{e}}}_{ij} = (\bar{\mathbf{v}}_i - \bar{\mathbf{v}}_j) / \left\|\bar{\mathbf{v}}_i - \bar{\mathbf{v}}_j\right\|$, the quantity

$$\beta^{is}(\bar{\mathbf{e}}_{ij}) = J(\nabla\phi|_{f_l} - \nabla\phi|_{f_k}) \cdot \hat{\bar{\mathbf{e}}}_{ij} \tag{2}$$

is the *signed isotropic angle* between the faces f_l and f_k. Positive values of $\beta^{is}(\bar{\mathbf{e}}_{ij})$ indicate compression in the bar $\bar{\mathbf{e}}_{ij}$. Note that $\beta^{is}(\bar{\mathbf{e}}_{ij}) = \beta^{is}(\bar{\mathbf{e}}_{ji})$.

3 Principal meshes in equilibrium

In this section we describe principal meshes in equilibrium under vertical loads. In Section 3.1, we show that these meshes are discretizations of special surfaces in membrane equilibrium, where principal directions of stress and curvature coincide. In Section 3.2, we first show how a membrane can be conveniently discretized with a triangular gridshell, enforcing the equilibrium on its edges. Then, we describe how to evaluate an equivalent stress tensor on a triangular gridshell and how to align the resultant principal directions with those of curvature. Finally, in Section 3.3, we outline our workflow to design principal meshes in equilibrium.

3.1 Principal stress and curvature alignment

Principal meshes are a discretization of the network of principal curvature lines of a continuous surface. A principal mesh in equilibrium, from a mechnanical point of view, is a gridshell with a quad combinatorics. At the limit of refinement, this gridshell will tend to a principal network of curves on a continuous surface in membrane equilibrium.

Let $\mathscr{M}(x,y)$ be a membrane under vertical load, parametrized as a height field surface over the xy plane, as described in Section 2.1. Let us then consider the principal network of curves of $\mathscr{M}(x,y)$, defined at each point by two tangent vectors $\mathbf{a}_1$ and $\mathbf{a}_2$, and let $\bar{\mathbf{a}}_1$ and $\bar{\mathbf{a}}_2$ be their xy projections. We are now looking for simple conditions which express that the principal network is in equilibrium.

First, for principal curve networks, the vectors $\mathbf{a}_1$, $\mathbf{a}_2$ follow principal curvature directions. These directions are orthogonal on the surface. With $\mathbb{I}$ as first fundamental form of $\mathscr{M}(x,y)$, we can express the orthogonality condition of $\mathbf{a}_1$, $\mathbf{a}_2$ as

$$\bar{\mathbf{a}}_1^T \mathbb{I} \bar{\mathbf{a}}_2 = 0. \tag{3}$$

Secondly, as seen in section 2.2, if a gridshell is in equilibrium under vertical loads, its xy projection must admit an Airy polyhedron Φ with planar faces. At the limit of refinement, the polyhedron Φ will tend to a continuous stress surface $z = \phi(x,y)$. For a quadrilateral gridshell, the corresponding Airy polyhedron is a quad mesh with planar faces. It is well known that a planar quad mesh, at the limit of refinement, will converge to a network of *conjugate curves* on a surface (Liu et al., 2006). We can then state the following condition: *a quad network on a surface is in horizontal equilibrium under vertical load if it is vertically projected onto a conjugate curve network on the corresponding Airy stress surface*. The condition for the directions $\mathbf{a}_1$, $\mathbf{a}_2$ to be vertically projected onto conjugate directions of $\phi(x,y)$ is expressed by

$$\bar{\mathbf{a}}_1^T \nabla^2 \phi \, \bar{\mathbf{a}}_2 = 0. \tag{4}$$

As shown in (Kilian et al., 2017), Equations (3) and (4) imply that the vectors $\bar{\mathbf{a}}_1$, $\bar{\mathbf{a}}_2$ are eigenvectors of $\mathbb{I}^{-1}\nabla^2\phi$. Since the principal stress directions on $\mathscr{M}(x,y)$ are given by the eigenvectors of $\Delta^{1/2}\mathbb{I}^{-1}\nabla^2\phi$, we can see that the only directions in horizontal equilibrium and orthogonal on the membrane are the principal stress directions. Therefore, we can state the following important fact:

Proposition 1. *Principal meshes in equilibrium under vertical loads are discrete representations of membrane surfaces where principal stress and principal curvature directions agree. There, they follow these principal directions.*

3.2 Estimating stress and curvature

As seen in section 2.1, at each point of a membrane we find three unknown stress components and three equilibrium equations. Membranes are then statically determinate in the sense that, given the loads and the boundary tractions, the stress tensor is uniquely determined; the existence of a solution depends only on the membrane geometry. Let us now consider a triangular gridshell forming a closed polyhedron Γ of genus zero, and with loads applied in its nodes. Denoting by v its number of vertices and e its number of edges, Euler's formula shows that $3v = e+6$. Since we have one unknown axial force per edge and three equilibrium equations per vertex, the solution is uniquely determined up to rigid body motion; the existence of the solution depends on the geometry of the polyhedron. The same is true for a portion of Γ, given the force reactions of the remaining part. Triangular gridshells can therefore reproduce the statical determinacy of membranes, see (Pavlovi, 1984). In the following, we express membrane behavior of a surface through the equilibrium of a gridshell triangulation.

In the continuous membrane, the projected stress tensor $\bar{S}$ and the isotropic shape operator $\nabla^2\phi$ are related by $\bar{S} = \widetilde{\nabla^2\phi}$. We are now searching for a discrete analog of the isotropic shape operator defined for triangle meshes, and at first look at the Euclidean counterpart. For that, we use the normal cycle approach by (Cohen-Steiner and Morvan, 2003). One computes an extended shape operator W (3×3 matrix with two eigenvectors in principal curvature direction and the third eigenvector, with eigenvalue close to zero, orthogonal to the surface) as follows. Selecting a vertex $\mathbf{v}_i$ and a surrounding region R_i of area A_i, W is found by

$$W(\mathbf{v}_i) = \frac{1}{A_i}\sum_{j\sim i}\beta(\mathbf{e}_{ij})\left\|\mathbf{e}_{ij}\cap R_i\right\|\hat{\mathbf{e}}_{ij}\hat{\mathbf{e}}_{ij}^T. \tag{5}$$

Here $\beta(\mathbf{e}_{ij})$ is the signed Euclidean angle between the two normals of the faces adjacent to the edge $\mathbf{e}_{ij}$, $\mathbf{e}_{ij}\cap R_i$ is the portion of the edge $\mathbf{e}_{ij}$ intersecting the region R_i and $\hat{\mathbf{e}}_{ij}$ is the unit edge vector, given by $(\mathbf{v}_i-\mathbf{v}_j)/\left\|\mathbf{v}_i-\mathbf{v}_j\right\|$. The eigenvalues of $W(\mathbf{v}_i)$, associated with the two eigenvectors lying in the tangent plane at $\mathbf{v}_i$, will give an estimation of principal curvatures along the swapped tangent eigenvectors. To obtain a discrete isotropic shape operator, we have to replace Euclidean quantities by isotropic ones. This means that lengths and areas are measured in the

xy plane and the Euclidean angle $\beta(\mathbf{e}_{ij})$ is replaced by the signed isotropic angle $\beta^{is}(\bar{\mathbf{e}}_{ij})$, given by Equation (2). Setting $\bar{\mathbf{e}}_{ij} \cap \bar{R}_i = \bar{\mathbf{v}}_i - \bar{\mathbf{v}}_j$, we can estimate the 2×2 adjoint Hessian of Φ at $\bar{\mathbf{v}}_i$ as

$$\widetilde{\nabla}^2 \phi(\bar{\mathbf{v}}_i) = \bar{S}(\bar{\mathbf{v}}_i) = \frac{1}{\bar{A}_i} \sum_{j \sim i} J(\nabla\phi|_{f_l} - \nabla\phi|_{f_k})(\bar{\mathbf{v}}_i - \bar{\mathbf{v}}_j)^T.$$

Observing that $J(\nabla\phi|_{f_l} - \nabla\phi|_{f_k}) = \bar{\mathbf{f}}_{ij} = w_{ij}(\bar{\mathbf{v}}_i - \bar{\mathbf{v}}_j)$, we can estimate the stress tensor directly through force densities as

$$\bar{S}(\bar{\mathbf{v}}_i) = \frac{1}{\bar{A}_i} \sum_{j \sim i} w_{ij}(\bar{\mathbf{v}}_i - \bar{\mathbf{v}}_j)(\bar{\mathbf{v}}_i - \bar{\mathbf{v}}_j)^T. \tag{6}$$

To estimate the principal curvature directions on the triangulated surface we use again Cohen-Steiner Equation (5). For sufficiently smooth meshes, we can make the approximation $\beta \approx \sin\beta$. With $\mathbf{n}_{f_k}$ and $\mathbf{n}_{f_l}$ as the unit normals of the left and right faces of the edge $\mathbf{e}_{ij}$, we can then estimate the 3×3 extended shape operator as

$$W(\mathbf{v}_i) = \frac{1}{A_i} \sum_{j \sim i} (\mathbf{n}_{f_l} \times \mathbf{n}_{f_k})(\mathbf{v}_i - \mathbf{v}_j)^T. \tag{7}$$

Let κ_1 and κ_2 be the eigenvalues of W corresponding to the two eigenvectors in the tangent plane of M. We can ensure the alignment of two vectors $\mathbf{a}_1$, $\mathbf{a}_2$ with principal directions at each vertex $\mathbf{v}_i$ by requiring

$$W\mathbf{a}_1 = \kappa_1 \mathbf{a}_1, \quad W\mathbf{a}_2 = \kappa_2 \mathbf{a}_2.$$

3.3 Workflow

We have now the elements to design principal meshes in equilibrium. In particular, we solve this problem: *Given an initial surface subject to gravitational load and its support conditions, find a quadrilateral mesh in force equilibrium with edges aligned along principal curvature directions that is close to the initial design surface*. Our procedure can be summarized in the following steps:

step 1. Given an input surface as a triangular mesh and the support conditions, we optimize the mesh geometry in order to align the equivalent stress and curvature directions as described in section 3.2, while keeping the vertices as close as possible to the input shape. The development and implementation of this step is the main contribution of this paper.

step 2. We use the resulting directions as guide for a quadrilateral remeshing of the optimized mesh. At this purpose we use *mixed integer quadrangulation* proposed by (Bommes et al., 2009). In this step, the density of the mesh can be chosen according to fabrication and design considerations.

step 3. The obtained quadrilateral mesh is subject to post-optimization for equilibrium and planarity of faces, while applying some fairness to the network curves to

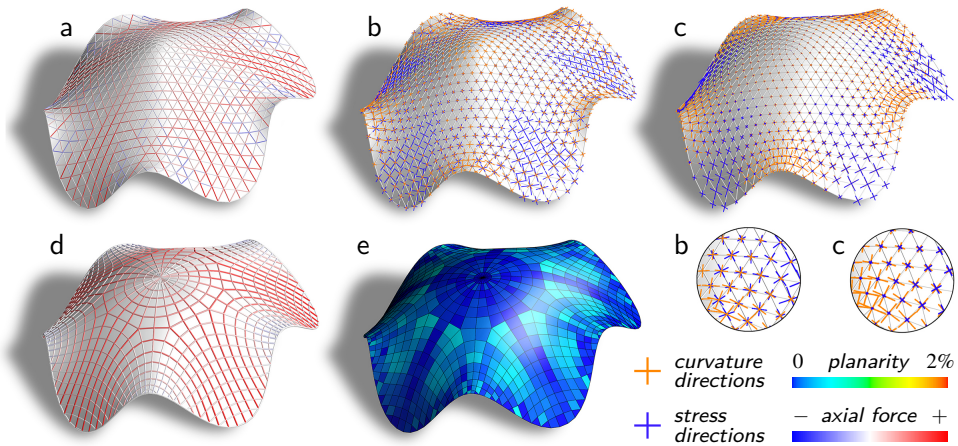

*Figure 3: Design workflow. (**a**) An initial shape is given as triangular mesh and the equilibrium is enforced on the edges. (**b**) The estimated curvature and stress directions, in general, are not aligned. (**c**) After our optimization, we reach the alignment with a change in the shape. (**d**) We remesh the resulting shape with mixed integer quadrangulation along the computed directions. After a post-optimization, the structure is in equilibrium under axial forces, (**e**) and panels are close to planar. According to a finite element analysis, the ratio of internal elastic work w_a due to axial forces in the final structure is 0.95. The stress and curvature directions are scaled according to their anisotropy, given by the difference between the two eigenvalues. A possible application of this design is depicted in Figures 1 and 7 (on the right).*

guarantee aesthetic quality. For this purpose, we use the method of (Tang et al., 2014). Thanks to *step 1*, we can expect convergence with minimized conflict between planarity and equilibrium.

4 Implementation

In this section we briefly describe the implementation of *step 1*, described in the workflow Section 3.3. Starting from a given triangular mesh M^0 with specified support conditions, we find a mesh M where principal stresses and principal curvature directions are aligned, as close as possible to M^0.

Main variables and constraints. For a mesh M^0 with v vertices and e edges, being s and c respectively the number of vertices that are mechanically supported, and fixed during the optimization, the main variables of the problem are:

- the position of the vertices $\mathbf{v}_i$ of M ($3(v-c)$ variables)
- the force densities $w_{ij} = w_{ji}$ (e variables)
- the components of the stress tensor $\bar{S}_{11}, \bar{S}_{22}$ and $\bar{S}_{12}$ ($3v$ variables)
- the components of the extended shape operator $W_{11}, W_{22}, W_{33}, W_{12}, W_{23}$ and W_{13} ($6v$ variables)

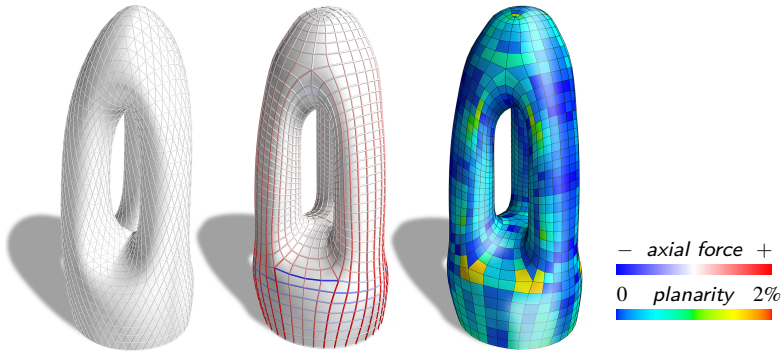

Figure 4: Results. A high-genus principal mesh in equilibrium. Finite element analysis showed an axial work ratio w_a of 0.89. On the left, the starting mesh M_0 is shown.

- the tangent eigenvalues κ_1 and κ_2 of the extended shape operator ($2v$ variables)
- the directions $\mathbf{a}_1$ and $\mathbf{a}_2$ at $\mathbf{v}_i$ ($6v$ variables).

The main constraints are:

- the equilibrium at unsupported vertices $\mathbf{v}_i$ through Equation (1) ($3(v-s)$ equations)
- the connection of the stress tensor components with force densities through Equation (6) ($3v$ equations). Since we are interested only in principal directions, we can omit $\bar{A}_i$ from the equations.
- the connection of the curvature components with face normals through Equation (7) ($6v$ equations). As for the previous point, we omit A_i.
- the normalization of directions: $\mathbf{a}_1^T\mathbf{a}_1 = 1$ and $\mathbf{a}_2^T\mathbf{a}_2 = 1$ ($2v$ equations)
- the tangency of directions (tangency is guaranteed together with principal direction alignment, see below): $(\mathbf{a}_1+\mathbf{a}_2)^T\mathbf{n}_i = 0$ (v equations)

where $\mathbf{n}_i$ is the vertex normal at $\mathbf{v}_i$. The target functions are given by the alignment equations of the vectors $\mathbf{a}_1, \mathbf{a}_2$ with stress and curvature directions, as seen in Sections 3.1 and 3.2. We have then:

- conjugacy on the Airy surface: $\bar{\mathbf{a}}_1^T\tilde{\bar{S}}\bar{\mathbf{a}}_2 = 0$ (v equations)
- principal direction alignment: $W\mathbf{a}_1 = \kappa_1\mathbf{a}_1$ and $W\mathbf{a}_2 = \kappa_2\mathbf{a}_2$ ($6v$ equations).

For proximity to the starting surface, we minimize the distance between the points $\mathbf{v}_i$ and the tangent plane of their closest vertex $\mathbf{v}_j^0$ of M^0. We point out here that the projected stress tensor $\bar{S}$ is not properly defined for surface points with a vertical tangent plane. To avoid noise in the solution, we remove the target functions of Airy conjugacy on vertices $\mathbf{v}_i$ where the z coordinate of the normal $\mathbf{n}_i$ is in the range $\pm 10^{-2}$.

Counting degrees of freedom. Subtracting the number of constraints from the number of variables, and keeping fixed during the optimization the supported vertices (then $s = c$), we find $5v + e$ degrees of freedom. The target functions of alignment yield $7v$ equations. Considering that on a triangle mesh we have $e \approx 3v$, we are left with approximately v degrees of freedom. This allows us to ask for closeness to the reference shape as a soft constraint.

Solver. For the optimization, we use the *guided projection* method of (Tang et al., 2014). This method works best for systems of quadratic constraints. To reduce the degree of the main constraints when higher than two, we introduce secondary variables that are quadratic functions of the main ones; then, these functions are added as constraints. Let us rearrange all the variables, in number of V, in the vector $\mathbf{x} \in \mathbb{R}^V$. Let then $\varphi_n(\mathbf{x}) = 0$, $n = \{1, \dots, N\}$, be the equations given by the constraints and the target functions. It is possible to add more or less importance to a specific constraint or target function by multiplying the corresponding equations by a weight ω_n. The system is solved iteratively. At each iteration k, given the current variable vector $\mathbf{x}^k$, each equation is linearized with a 1st order Taylor expansion:

$$\varphi_n(\mathbf{x}) \approx \varphi_n(\mathbf{x}^k) + \nabla\varphi_n(\mathbf{x}^k)^T(\mathbf{x} - \mathbf{x}^k) = 0.$$

The linearized system of weighted equations can be rearranged in matrix form as $H\mathbf{x} = \mathbf{r}$, with $H \in \mathbb{R}^{N \times V}$ and $\mathbf{r} \in \mathbb{R}^N$. To guarantee mesh quality and smoothness during the optimization, we add a fairness energy; we define it at each vertex $\mathbf{v}_i$ as the squared norm of the distance between $\mathbf{v}_i$ and the barycenter of its connected vertices $\mathbf{v}_{j \sim i}$. The total fairness energy can be written in matrix form as $\|K\mathbf{x} - \mathbf{s}\|^2$. Additionally, the distance from $\mathbf{x}^k$ is used as a regularizer. The successive variable vector $\mathbf{x}^{k+1}$ is found by solving

$$\|H\mathbf{x} - \mathbf{r}\|^2 + \delta^2 \|K\mathbf{x} - \mathbf{s}\|^2 + \varepsilon^2 \left\|\mathbf{x} - \mathbf{x}^k\right\|^2 \to \min,$$

with $\delta, \varepsilon \in (0,1)$ as weights. The iteration stops when a desired accuracy is achieved, or when no more improvement is gained. For further details on *guided projection*, we refer to (Tang et al., 2014).

Fig.	v	e	iterations	time (s)
3	681	1960	12	13.8
4	1941	5784	15	78.4
5a	606	1760	15	16.7
5b	1140	3302	14	31.9
5c	1089	3136	13	28.3

Table 1: Optimization times and corresponding number of iterations for stress and curvature alignment, relative to the presented results. Values refer to triangular meshes with v vertices and e edges. The algorithm has been implemented in Python and tested with an Intel Core i7-6700HQ CPU with 2.60 GHz and a 15.9 GB RAM memory.

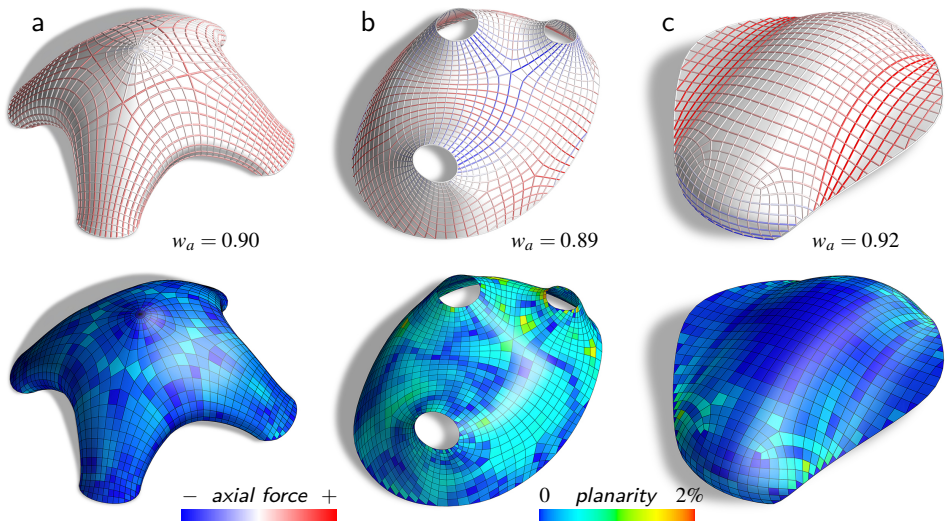

*Figure 5: Results. Principal meshes in equilibrium achieved with our method. Meshes (**a**) and (**c**) discretize non-height field shapes. All boundaries are supported. The gridshell structures are in axial equilibrium under a homogeneous vertical load per unit surface area. Axial forces, planarity error and axial work ratios w_a are shown.*

5 Results and discussion

The proposed workflow has been tested on some sample architectural surfaces. Results are shown in Figures 3 to 5. The presented examples were subject to a uniform load per unit surface area and supported along the boundary. Optimization times of *step 1* are given in Table 1. To evaluate the quality of the result, we relied on the following two criteria.

Convergence of post-optimization. As seen in Section 3.3, the quad mesh is post-optimized for equilibrium and planarity with the method of (Tang et al., 2014). In this step, we let the supported vertices glide along the corresponding boundary. We estimated planarity error of quadrilateral faces as the distance between the two face diagonals divided by their mean length. Regarding equilibrium, we evaluated the error per vertex as the norm of equilibrium Equation (1) divided by the mean vertex load magnitude. We considered the post-optimization converged when it reached a maximum planarity error below 2% and a mean equilibrium error below 1%. In the test samples we achieved convergence in less than ten iterations, noticing small changes in the mesh.

Finite element analysis. In actual gridshells the structure is dimensioned according to finite element analysis. It is of interest to evaluate the effectiveness of our optimization in this way as well. For this purpose, we modeled the final grid shell with steel S235 Timoshenko beam elements, connected together with rigid joints. Area loads were lumped in the nodes. The size of the cross section was chosen constant, according to resistance verification. To evaluate the equilibrium

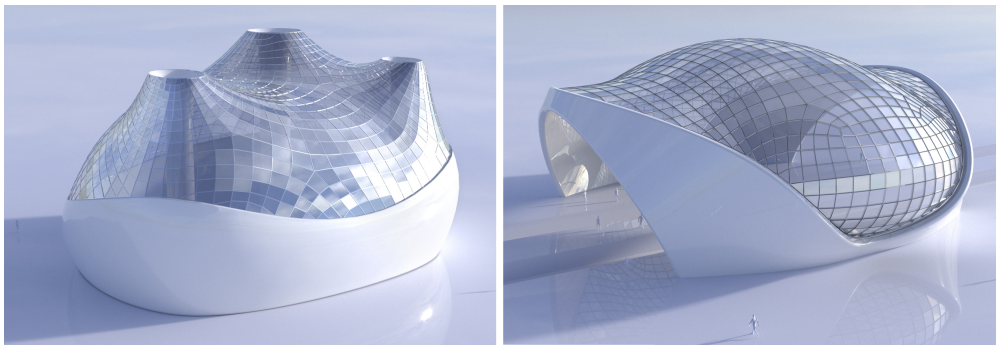

Figure 6: Architectural applications. Steel-glass gridshells achievable with the meshes shown in Figures 5b (on the left) and 5c (on the right). Face planarity errors below 2% are compatible with cladding through flat glass panels.

hypothesis, we computed the ratio of internal elastic work due to axial force in the beams over the total elastic work made by external loads. Axial work ratios w_a, found for our results, are shown beside Figures 3 to 5.

Limitations. Not all shapes achievable with our method own a stress-curvature network suitable for the extraction of architectural meshes. Indeed, the network layout may yield a mesh with a large variation of cell size, numerous or bad positioned singularities, or more generally, the resulting mesh may not possess the desired aesthetic qualities.

6 Conclusion

We have introduced a method for the design of principal meshes in equilibrium. Thanks to the optimization of a membrane surface towards stress and curvature alignment, we can achieve a quad mesh connectivity that can be post-optimized for equilibrium and planarity of faces with low conflict. In our implementation, the use of a discrete equilibrium on the edges of a triangular mesh allows us to avoid a parametrization of the surface and the explicit use of an Airy stress function. We have overcome in this way the limitations to height field shapes of (Kilian et al., 2017). We provide then a tool for the design of a wide range of architectural freeform shapes that, taking into account geometric and static factors, can reduce realization costs.

Acknowledgments

This research was supported by SFB-Transregio programme Geometry and Discretization (Austrian Science Fund grant no. I 2978), and by the project "Geometry and Computational Design for Architecture and Fabrication" at Vienna University of Technology.

References

Angelillo, M. and A. Fortunato (2004). Equilibrium of masonry vaults. In M. Fremond and F. Maceri (Eds.), *Novel Approaches in Civil Engineering*, pp. 106–111. Oxford: Springer.

Block, P. and J. Ochsendorf (2007). Thrust network analysis: A new methodology for three-dimensional equilibrium. *Journal of International Association for Shell and Spatial Structures 48*(3), 167–173.

Bommes, D., H. Zimmer, and L. Kobbelt (2009). Mixed-integer quadrangulation. *ACM Transactions on Graphics 28*(3), 77:1–77:10.

Cohen-Steiner, D. and J. M. Morvan (2003). Restricted Delaunay triangulations and normal cycle. In *Proceedings of the Nineteenth Annual Symposium on Computational Geometry*, New York, pp. 312–321. ACM.

Fraternali, F. (2010). A thrust network approach to the equilibrium problem of unreinforced masonry vaults via polyhedral stress functions. *Mechanics Research Communications 37*(2), 198–204.

Kilian, M., D. Pellis, J. Wallner, and H. Pottmann (2017). Material-minimizing forms and structures. *ACM Transactions on Graphics 36*(6), 173:1–173:12. Proc. SIGGRAPH Asia.

Liu, Y., H. Pottmann, J. Wallner, Y.-L. Yang, and W. Wang (2006). Geometric modeling with conical meshes and developable surfaces. *ACM Transactions on Graphics 25*(3), 681–689. Proc. SIGGRAPH.

Maxwell, J. C. (1872). On reciprocal figures, frames, and diagrams of forces. *Transactions of the Royal Society of Edinburgh 26*, 1–40.

Mitchell, T. (2013). *A Limit of economy of material in shell structures*. Ph. D. thesis, University of California, Berkeley.

Pavlovi, M. (1984). A statically determinate truss model for thin shells: One-surface analysis (membrane hypothesis). *International Journal for Numerical Methods in Engineering 20*(10), 1841–1861.

Pottmann, H., M. Eigensatz, A. Vaxman, and J. Wallner (2015). Architectural geometry. *Computers and Graphics 47*, 145–164.

Pottmann, H. and Y. Liu (2007). Discrete surfaces in isotropic geometry. In R. Martin, M. Sabin, and J. Winkler (Eds.), *Mathematics of Surface XII*, Volume XII, pp. 431–363. Springer.

Schiftner, A. and J. Balzer (2010). Statics-sensitive layout of planar quadrilateral meshes. In C. Ceccato et al. (Eds.), *Advances in Architectural Geometry 2010*, pp. 221–236. Springer.

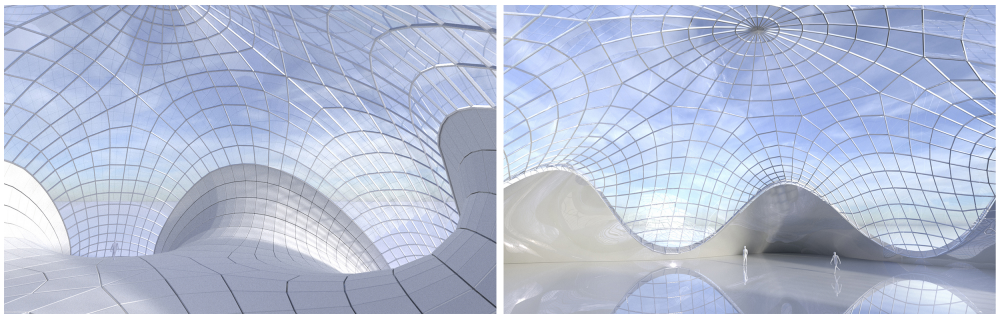

Figure 7: Architectural applications. Interior views of the meshes shown in Figures 5a (on the left) and 3 (on the right). Exterior views are shown in Figure 1.

Sun, X. (2016). *Discrete Curvature Theories and Applications*. Ph. D. thesis, King Abdullah University of Science and Technology, Thuwal.

Tang, C., X. Sun, A. Gomes, J. Wallner, and H. Pottmann (2014). Form-finding with polyhedral meshes made simple. *ACM Transactions on Graphics 33*(4), 70:1–70:9.

Vouga, E., M. Höbinger, J. Wallner, and H. Pottmann (2012). Design of self-supporting surfaces. *ACM Transactions on Graphics 31*(4), 87:1–87:11.